

The Paramagnetic Resonance Spectra of Spin Labels in Phospholipid Membranes

BETTY JEAN GAFFNEY* AND HARDEN M. MCCONNELL

Stauffer Laboratory for Physical Chemistry, Stanford University, Stanford, California 94305

Received January 7, 1974

An analysis of the paramagnetic resonance spectra of phospholipid spin labels incorporated in phospholipid bilayer membranes is described. The analysis takes into account rapid anisotropic motion which gives rise to an effective spin Hamiltonian. The broadening of transitions between the eigenstates of this effective Hamiltonian is approximated using Redfield relaxation theory. The analysis of the spectra also takes into account spacial distributions of the axes of the effective spin Hamiltonian as well as a field-induced orientation of the lipid molecules. Resonance spectra are reported for isotropic samples, as well as oriented multibilayers (smectic liquid crystals), at 9.3 and 35.0 GHz, for various orientations of the applied field. Order parameters for the phospholipid spin labels are determined, and calculations are made of order parameters appropriate to different types of spectroscopic time-averaging, including ensemble-average order parameters that correspond to long-time averages.

INTRODUCTION

The paramagnetic resonance spectra of nitroxide spin labels have provided novel information about kinetic and structural properties of biological membranes, and model membranes (phospholipid bilayers) (1). This information has included direct evidence for hydrophobic regions of low local viscosity (2), the flexibility gradient in spin-labeled fatty acid chains (3-8), high rates of lateral diffusion of phospholipids (9-13), and rates of transmembrane motion (14). In much of this work, a quantitative, or semiquantitative, analysis of the paramagnetic resonance spectra of spin-labeled fatty acids, or spin-labeled phospholipids, has been used. In the present paper, we summarize our analysis of the spectra of spin labels in phospholipid membranes where there is no interaction between the labels because they are present in low concentration (e.g., 0.1-1 mole %). This type of analysis may also be useful for studies of the paramagnetic resonance spectra of spin labels attached to proteins in membranes.

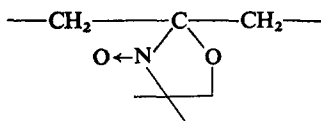
THE SPIN HAMILTONIAN

In standard notation, the spin Hamiltonian for a nitroxide spin label is [1]

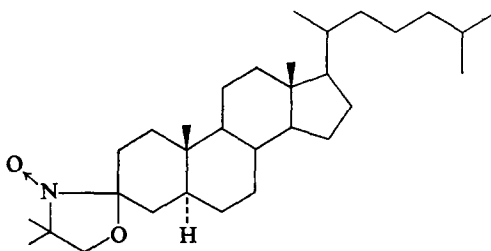
$$\mathcal{H} = |\beta|S \cdot g \cdot H_0 + hS \cdot T \cdot I + \beta_N g_N I \cdot H_0, \quad [1]$$

* Present address: Department of Chemistry, The Johns Hopkins University, Baltimore, Maryland 21218.

where **I** refers to the ^{14}N nuclear spin of the $\text{N} \rightarrow \text{O}$ group. The spin labels considered here all contain the five-membered oxazolidine ring:



One set of values for the elements of the **g** and **T** dyadics has been obtained from an analysis of the paramagnetic resonance spectra of the cholesterol spin label **I**



I

in single crystals of cholesteryl chloride (3). This study has recently been repeated with great precision by Dr. R. C. McCalley in this laboratory, who has found the **g** and **T** tensor elements given in Table 1. As reported in earlier work, the *z*-direction is parallel to the π -orbital of the nitrogen atom, and *x* is along the $\text{N}-\text{O}$ bond direction (3). In

TABLE 1
TENSOR ELEMENTS^a

| Label | T_{zz} | T_{xx} | T_{yy} | g_{zz} | g_{xx} | g_{yy} |
|---------------------------------|-----------------|----------------|----------------|---------------------|---------------------|---------------------|
| Cholesterol spin label I | 89.4 ± 0.06 | 17.7 ± 0.3 | 16.4 ± 0.3 | 2.0024 ± 0.0001 | 2.0090 ± 0.0001 | 2.0060 ± 0.0001 |
| II (10,3) | 93.8 | 17.6 | 16.3 | 2.0027 | 2.0088 | 2.0061 |

^a Data for spin label **I** obtained by R. C. McCalley in this laboratory. Elements of the hyperfine tensor **T** are in MHz.

McCalley's work it was established that the principal axis systems of the **g**- and **T**-tensors are parallel to within a few degrees, or less. These small angular deviations may be due to host crystal effects.

In the analysis of the paramagnetic resonance spectra of spin labels in biological systems, one must often determine the elements of the spin Hamiltonian from imperfectly oriented samples. An analysis of this type is illustrated in Fig. 1, which shows observed and calculated spectra for the spin label **II**(10,3) bound to a lyophilized sample of bovine serum albumin, at 9.3 and 35.0 GHz.

T-tensors. This sensitivity is especially high when agreement with both low- and high-field spectra is required. We believe that much of the deviation between the observed and calculated spectra can be attributed to the fact that the single-orientation resonance signals are not exactly Lorentzian, but are partially Gaussian. Evidence for Gaussian contributions to the line shape is described below.

It has been shown previously (3, 15) that the outer wings of the derivative curves at 9.3 GHz provide an approximate measure of the absorption line shapes themselves. Figure 2 illustrates the high- and low-field extrema at 9.3 GHz for $\text{II}(10,3)$ in lyophilized

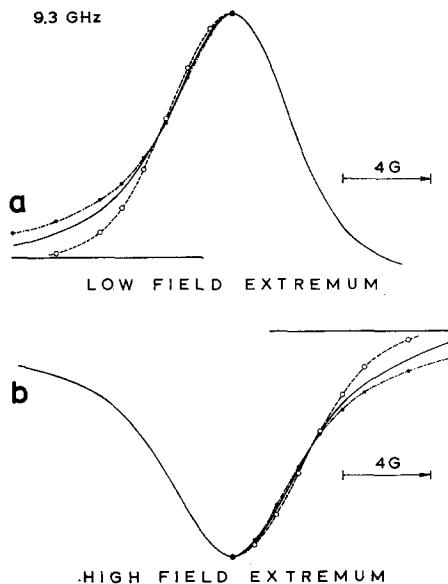


FIG. 2. (a) The experimental low-field extremum of the 9.3-GHz paramagnetic resonance spectrum shown in Fig. 1(a) (solid line —) is superimposed on calculated Gaussian (----) and Lorentzian (-.-.-) absorption curves. The Gaussian and Lorentzian curves were calculated using a half-height width of 18.48 MHz. (b) As in (a) except the high-field extremum is shown. The Gaussian and Lorentzian absorption curves were calculated using a half-height width of 20.72 MHz.

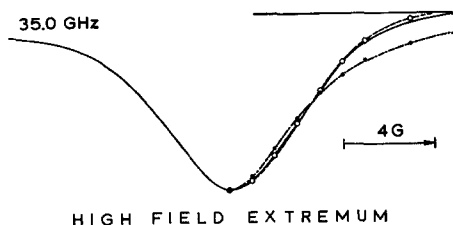


FIG. 3. The high-field extremum of the experimental 35.0-GHz paramagnetic resonance spectrum shown in Fig. 1(b) is superimposed on calculated Gaussian (----) and Lorentzian (-.-.-) absorption curves. The Gaussian and Lorentzian curves were calculated using a half-height width of 20.72 MHz.

bovine serum albumin; for comparison pure Lorentzian and Gaussian lines are shown, and it is seen that the observed signals are intermediate between the two. The high-field extremum at 35.0 GHz is well-resolved and is nearly Gaussian in shape, as illustrated in Fig. 3.

THE EFFECTS OF MOTION AND ORIENTATION

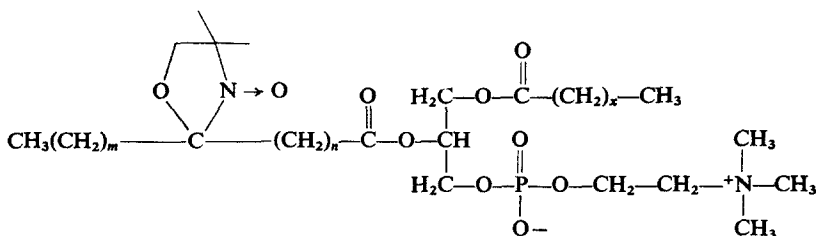
In earlier publications we and others have interpreted the paramagnetic resonance spectra of spin labels incorporated in membranes in terms of an effective, time-average spin Hamiltonian, \mathcal{H}' (2). That is, in the presence of molecular motion, the Hamiltonian becomes time dependent and is written in terms of time-dependent and time-independent parts:

$$\mathcal{H}(t) = \mathcal{H}' + [\mathcal{H}(t) - \mathcal{H}']. \quad [2]$$

In calculations of resonance spectra, it has been assumed that $[\mathcal{H}(t) - \mathcal{H}']$ acts as a high-frequency perturbation that can be treated by perturbation theory (e.g., Redfield theory (16)). This perturbation then leads to Lorentzian contributions to the linewidths. As discussed below, a time-dependent perturbation of this type leads to anisotropic resonance linewidths, that is, linewidths that depend on the orientation of the applied field relative to the principal axes of \mathcal{H}' , namely, x' , y' , and z' .

The utility and accuracy of the decomposition, Eq. [2], can only be established by detailed comparisons between observed and calculated spectra. Phospholipid bilayers, in the smectic liquid-crystal state, enable one to obtain both isotropic and partially ordered distributions of spin labels and thus isotropic and partially ordered distributions of the axes x' , y' , z' of the effective spin Hamiltonian \mathcal{H}' . Comparisons between observed and calculated isotropic spectra designed to test Eq. [2] have the great advantage that the distribution of the axes x' , y' , z' is known precisely; such comparisons have the weakness that high-frequency, low-amplitude anisotropic motions can have certain effects on spectra that are qualitatively similar to the effects of slow, isotropic rotational diffusion (17). On the other hand, the anisotropy of the resonance spectra of partially oriented samples provides much more data for testing the adequacy of Eq. [2], but has the drawback that some functional form for the spatial distribution of the axes x' , y' , z' must be assumed, and the appropriate parameters of these distribution functions must be determined from the anisotropy of the resonance spectra. However, when calculations of both isotropic and anisotropic resonance spectra can be brought into accord with one another with reasonable assumptions about the spatial distribution functions, the evidence for the accuracy of the decomposition Eq. [2] becomes much stronger. Further tests of the theory can be made by comparisons of spectra at different field strengths, as described in the present paper, and under various conditions of microwave power saturation and field modulation, as will be discussed elsewhere. In the present work, small errors in the decomposition Eq. [2] may possibly be absorbed into our linewidth parameters or into the orientational distribution functions, and it is left to further work to see if such errors exist and if they are significant.

The labels of greatest interest in our work are the phospholipid spin labels **III**(m, n), $x \simeq m + n + 1$ (derived from egg lecithin):



III (m, n)

The Hamiltonian [1] can be expressed in terms of irreducible (tensor) dyadics \mathbf{F}_q , which are given in Table 2:

$$\mathbf{T} = a\mathbf{U} + \sum_q A_q \mathbf{F}_q, \quad [3]$$

$$\mathbf{g} = \bar{g}\mathbf{U} + \sum_q G_q \mathbf{F}_q \quad [4]$$

Here a and \bar{g} are the isotropic (average) hyperfine coupling constants and g -factor coupling constants, respectively and \mathbf{U} is the unit dyadic, $\mathbf{U} = \mathbf{ii} + \mathbf{jj} + \mathbf{kk}$. Explicit expressions for \mathbf{F}_q , A_q , and G_q are given in Table 2. The dyadics \mathbf{T} and \mathbf{g} are molecule-fixed; comparable

TABLE 2
IRREDUCIBLE DYADICS AND PARAMETERS

| |
|---|
| $\mathbf{F}_2 = (\mathbf{i} + \sqrt{-1}\mathbf{j})(\mathbf{i} + \sqrt{-1}\mathbf{j})$ |
| $\mathbf{F}_1 = -\mathbf{k}(\mathbf{i} + \sqrt{-1}\mathbf{j}) - (\mathbf{i} + \sqrt{-1}\mathbf{j})\mathbf{k}$ |
| $\mathbf{F}_0 = \sqrt{\frac{2}{3}}(3\mathbf{kk} - \mathbf{U})$ |
| $\mathbf{F}_{-1} = \mathbf{k}(\mathbf{i} - \sqrt{-1}\mathbf{j}) + (\mathbf{i} - \sqrt{-1}\mathbf{j})\mathbf{k}$ |
| $\mathbf{F}_{-2} = (\mathbf{i} - \sqrt{-1}\mathbf{j})(\mathbf{i} - \sqrt{-1}\mathbf{j})$ |
| $G_0 = \frac{1}{3}\sqrt{\frac{2}{3}}[g_{zz} - \frac{1}{2}(g_{xx} - g_{yy})]$ |
| $G_{\pm 1} = 0$ |
| $G_{\pm 2} = \frac{1}{4}[g_{xx} - g_{yy}]$ |
| $A_0 = \frac{1}{3}\sqrt{\frac{2}{3}}[T_{zz} - \frac{1}{2}(T_{xx} + T_{yy})]$ |
| $A_{\pm 1} = 0$ |
| $A_{\pm 2} = \frac{1}{4}[T_{xx} - T_{yy}]$ |

expressions hold for the effective Hamiltonian \mathcal{H}' and the dyadics \mathbf{T}' , \mathbf{g}' , and \mathbf{F}'_q that refer to the effective axis system x' , y' , z' . The molecule-fixed dyadics \mathbf{F}_q are related to the dyadics \mathbf{F}'_q by means of the Wigner rotation matrices:

$$\mathbf{F}_m = \sum_q D_{mq}(\alpha\beta\gamma) \mathbf{F}'_q. \quad [5]$$

Here α , β , γ , are the Eulerian angles that rotate the x' , y' , z' ($\mathbf{i}'\mathbf{j}'\mathbf{k}'$) axis system into the x , y , z (\mathbf{ijk}) axis system, as sketched in Fig. 4.

The hyperfine and g -tensors of the effective Hamiltonian can thus be written

$$\mathbf{T}' = a\mathbf{U} + \sum_{m,q} A_m \overline{D_{mq}(\alpha\beta\gamma)} \mathbf{F}'_q, \quad [6]$$

$$\mathbf{g}' = \bar{g}\mathbf{U} + \sum_{m,q} G_m \overline{D_{mq}(\alpha\beta\gamma)} \mathbf{F}'_q, \quad [7]$$

where $\overline{D_{mq}(\alpha\beta\gamma)}$ refers to a time-average over molecular motions of x , y , z relative to x' , y' , z' , which produce a time-dependence of α , β , γ . When the hyperfine and g -tensors of the effective Hamiltonian are written in terms of the new parameters A'_q and G'_q

$$\mathbf{T}' = a\mathbf{U} + \sum_q A'_q \mathbf{F}'_q, \quad [8]$$

$$\mathbf{g}' = \bar{g}\mathbf{U} + \sum_q G'_q \mathbf{F}'_q, \quad [9]$$

it follows that the terms A'_q and G'_q are related to A_q and G_q by time-averages over the rotation matrices:

$$A'_q = \sum_m A_m \overline{D_{mq}(\alpha\beta\gamma)}, \quad [10]$$

$$G'_q = \sum_m G_m \overline{D_{mq}(\alpha\beta\gamma)}. \quad [11]$$

As shown later, a consistent result that we have obtained in all of our studies of the fatty acid labels $\mathbf{II}(m,n)$ and phospholipid labels $\mathbf{III}(m,n)$ is that the effective Hamiltonian \mathcal{H}' has axial symmetry, to a very good approximation, even when \mathbf{T}' and \mathbf{g}' are

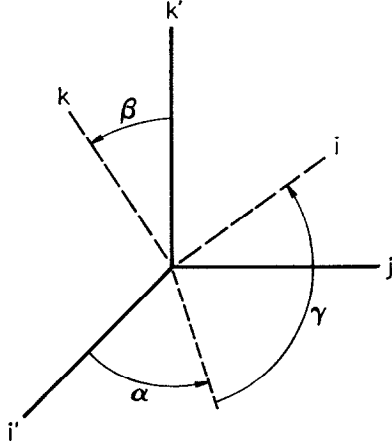


FIG. 4. The molecule-fixed axis system $x, y, z(i, j, k)$ and the effective axis system $x', y', z'(i', j', k')$. The angles α, β, γ , are the Eulerian angles that rotate the i', j', k' system into the i, j, k system.

far from isotropic (e.g., as in the case of $\mathbf{II}(10,3)$ and $\mathbf{III}(10,3)$). This implies that the elements G'_2, G'_{-2} and A'_2, A'_{-2} are zero, which can be achieved by averaging motions involving the Eulerian angles α and γ .

The axial symmetry of the effective Hamiltonian \mathcal{H}' does *not* imply that there is any symmetry or equivalence among the order parameters $S_{k'k}, S_{k'i}, S_{k'j}$, where

$$S_{k'k} = \frac{1}{2}(3[\mathbf{k}' \cdot \mathbf{k}]^2 - 1), \quad [12]$$

$$S_{k'i} = \frac{1}{2}(3[\mathbf{k}' \cdot \mathbf{i}]^2 - 1), \quad [13]$$

$$S_{k'j} = \frac{1}{2}(3[\mathbf{k}' \cdot \mathbf{j}]^2 - 1), \quad [14]$$

and where

$$\mathbf{k}' \cdot \mathbf{k} = \cos \beta, \quad [15]$$

$$\mathbf{k}' \cdot \mathbf{i} = \sin \beta \sin \gamma, \quad [16]$$

$$\mathbf{k}' \cdot \mathbf{j} = \sin \beta \cos \gamma. \quad [17]$$

The order parameter $S_{kk'}$ can be obtained most conveniently from the experimental determination of the elements of \mathbf{T} , namely T'_\parallel and T'_\perp , the values of \mathbf{T} parallel and perpendicular to k' (\mathcal{H}' having axial symmetry). In this case one can readily obtain the following equation from Eqs. [5] and [12]–[17]:

$$\frac{T'_\parallel - T'_\perp}{T_{zz} - \frac{1}{2}(T_{xx} + T_{yy})} = S_{k'k} + \frac{1}{2} \frac{(T_{xx} - T_{yy})(2S_{k'i} + S_{k'k})}{T_{zz} - \frac{1}{2}(T_{xx} + T_{yy})}. \quad [18]$$

For the parameters given in Table 1, it can be seen that the second term on the right-hand side of Eq. [18] must be of the order of 0.01 or less, and can be neglected in calculations of the order parameter $S_{kk'}$ when $S_{kk'}$ is greater than 0.1, as in the present work. An equation analogous to Eq. [18] holds for the g -factor:

$$\frac{g'_{\parallel} - g'_{\perp}}{g_{zz} - \frac{1}{2}(g_{xx} + g_{yy})} = S_{k'k} + \frac{1}{2} \frac{(g_{xx} - g_{yy})(2S_{k'i} + S_{k'k})}{(g_{zz} - \frac{1}{2}(g_{xx} + g_{yy}))} \quad [19]$$

Here the factor $g_{xx} - g_{yy}$ is not small compared to $g'_{\parallel} - g'_{\perp}$. Thus, when $S_{kk'}$ is determined from the hyperfine interactions, Eq. [19] can be used to determine the other order parameters $S_{k'i}$ and $S_{k'j}$, using the relation

$$S_{k'i} + S_{k'j} + S_{k'k} = 0. \quad [20]$$

In the present work we have found consistently that the best values of $g'_{\parallel} - g'_{\perp}$ to be used in calculating spectra are just those for which $(g'_{\parallel} - g'_{\perp}) / (g_{zz} - \frac{1}{2}(g_{xx} + g_{yy}))$ is equal to the $S_{kk'}$ obtained from hyperfine splitting data. From Eq. [19] this implies that $S_{k'i} \simeq -\frac{1}{2}S_{k'k}$. From Eq. [20] it follows further that $S_{k'i} \simeq S_{k'j}$ for the phospholipid labels discussed here. We conclude from our data that the order-parameter matrix does have approximate axial symmetry.

The eigenenergies of \mathcal{H}' are determined by the angle Θ between the applied field direction $\mathbf{h}(=\mathbf{H}_0/|\mathbf{H}_0|)$ and the principal axis z' , using standard formulas (3). In our calculations we have neglected the ^{14}N nuclear Zeeman term, $g_N \beta_N \mathbf{I} \cdot \mathbf{H}_0$, since even at 35 GHz ($H_0 \simeq 12,400$ gauss), this interaction is only of the order of 3 MHz and is thus small compared to the hyperfine interaction. Moreover, the effect of this term is totally negligible for the important cases where H_0 is perpendicular or parallel to z' .

The observed spectra thus depend on the eigenvalues of \mathcal{H}' , the distribution of the axes z' relative to the field direction, and the resonance linewidths appropriate to each orientation of the field in the molecular axis systems x' , y' , z' .

We have used two distribution functions for the principal axis z' , given below.

$$\rho(\vartheta) = \sin \vartheta \exp[-(\vartheta - \bar{\vartheta})^2 / 2\vartheta_0^2], \quad [21]$$

$$\rho(\vartheta, \varphi) = \sin \vartheta \{ \exp[-(\vartheta - \bar{\vartheta})^2 / 2\vartheta_0^2] \} \{ \exp[-\varphi^2 / 2\varphi_0^2] \}. \quad [22]$$

Here ϑ is the angle between z' and the normal \mathbf{N} to the bilayer membrane. (See Fig. 5). The distribution function containing φ allows for the possibility that the applied field itself induces an orientation of the phospholipid molecules in the plane of the membrane (18). In an axis system fixed in the bilayer plane, ϑ' and φ' are the polar and azimuthal angles of the field direction, and the direction $\varphi' = 0$ (and certain symmetry equivalent orientations) corresponds to the most probable direction of the component of z' in the plane of the bilayer. The field-induced orientation of the phospholipid molecules is discussed later.

The most unsatisfactory *theoretical* aspects of the entire calculation are the resonance linewidths. The time-dependent perturbation [$\mathcal{H}(t) - \mathcal{H}'$], when treated by time-dependent perturbation theory (Redfield theory), yields a Lorentzian contribution (T_2^{-1}) to the total linewidth that is given in the Appendix. It is clear that this "Redfield contribution" to the linewidths is not the only source of line broadening. Proton nuclear hyperfine structure certainly makes an inhomogeneous contribution to the linewidths, as does also the inhomogeneity due to the distribution of orientations. Fortunately,

as seen in the following discussions, different approximations for the resonance linewidths do not significantly affect the major conclusions from our studies.

In the following sections of the present paper, we describe a series of approximations used for computer-calculated spectra, each successive set of approximations being more elaborate in terms of allowing for more physical effects and including more parameters. These are approximations A, A', B, and B'. In all of these calculations, a single set of

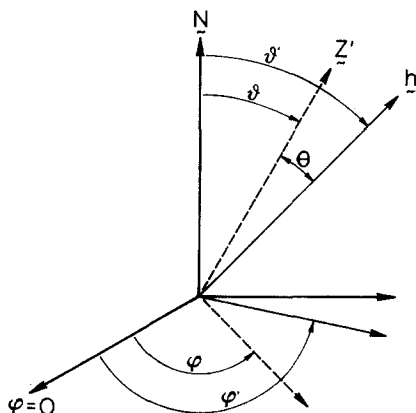


FIG. 5. The axis system which defines the orientation of the molecular z' axis relative to the magnetic field direction h . The normal to the sample plane (planes of phospholipid bilayers) is designated N .

parameters for the effective spin Hamiltonian \mathcal{H}' is used, as given in Table 3. Approximations C illustrate spectra calculated when deviations of \mathcal{H}' from axial symmetry are considered; this provides further evidence supporting our conclusion that the approximate effective Hamiltonians \mathcal{H}' do have axial symmetry.

TABLE 3

PARAMETERS USED FOR CALCULATION OF PARAMAGNETIC RESONANCE SPECTRA FOR PHOSPHOLIPID SPIN LABELS IN LECTHIN BILAYERS^a

| Label | III(10,3) | III(7,6) | III(5,10) | III(1,14) |
|----------------------------|-----------|----------|-----------|-----------|
| T'_i (MHz) | 76.8 | 70.8 | 56.0 | 46.5 |
| T'_l (MHz) | 25.5 | 28.5 | 32.2 | 35.6 |
| $g'_i - g'_l$ ^b | -0.0033 | -0.0027 | -0.0016 | -0.0010 |

^a The same parameters were used for calculations of 9.3 and 35.0 GHz spectra.

^b $g'_i - g'_l$ can be estimated from the difference, δ , between the center points of the outer hyperfine extrema (separation $2T'_i$) and the inner extrema (separation $2T'_l$) of the paramagnetic resonance spectrum of an isotropic distribution of labeled bilayers:

$$g'_i - g'_l = \frac{-\delta}{H_0} \times 2.0023.$$

9.3 GHz

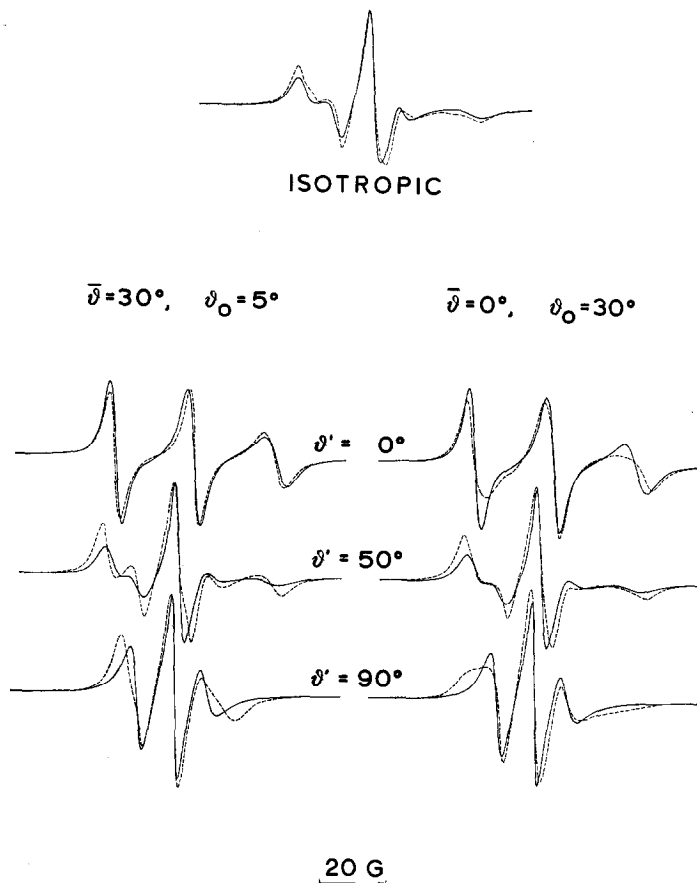


FIG. 6. Comparison of experimental (solid line) and calculated (dashed line) paramagnetic resonance spectra at 9.3 GHz for the lecithin spin label III(10,3) in hydrated bilayers of egg lecithin at 25°C. The ratio of spin-labeled lecithin to egg lecithin molecules is 1 to 100. The experimental isotropic spectrum was obtained from a distribution of hydrated bilayers on a hemispherical surface. The oriented spectra were obtained from a sample of hydrated bilayers oriented by shear between two quartz plates ($\sim 1 \times 4$ cm). For both samples, temperature and humidity were controlled by a stream of nitrogen moistened by bubbling through a saturated aqueous solution of potassium bromide before entering the microwave cavity of the spectrometer. Experimental spectra are shown for three orientations ($\vartheta' = 0, 50, 90^\circ$) of the magnetic field direction relative to the normal to the glass plates (normal to bilayer planes). The parameters given for III(10,3) in Table 3 were used for the calculated spectra. A set of spectra are shown assuming a net tilt of the long chain axes ($\bar{\vartheta} = 30^\circ, \vartheta_0 = 5^\circ$) and no tilt ($\bar{\vartheta} = 0, \vartheta_0 = 30^\circ$). Approximation A was used for the calculations. Peak-to-trough derivative-curve linewidths are $A(1) = 9.8, A(0) = 9.8, A(-1) = 14$ MHz.

APPROXIMATIONS A

This series of approximations, enumerated below, is the simplest that can be made which provides reasonable representations of the observed spectra. Except for (A-4), these approximations were originally made by Hubbell and McConnell (3) for calculations for isotropic distributions.

- (A-1) The effective spin Hamiltonian \mathcal{H}' has axial symmetry.
- (A-2) The line shape for each hyperfine signal is Lorentzian. (Gaussian and Gaussian–Lorentzian mixtures have also been used but are not discussed here.)
- (A-3) The linewidth for each hyperfine signal is isotropic; but m -dependent, where m is the component of the nitrogen nuclear spin in the local field direction at the nucleus.
- (A-4) The spacial distribution of the average principal hyperfine axis in oriented multibilayers is given by Eq. [21].

The linewidths were chosen for optimum fit of computed spectra to experimental spectra for $\vartheta' = 0$ and for the isotropic distribution. The best fit to the $\vartheta' = 0$ spectrum was obtained for $\bar{\vartheta} = 30^\circ$, $\vartheta_0 = 5^\circ$, for variations of $\bar{\vartheta} = 0, 10, 20, 30, 40^\circ$ as well as variations of ϑ_0 . Spectra are shown in Fig. 6 for 9.3 GHz. The best fit for $\bar{\vartheta} = 0$ is also shown, and it is seen that a large ϑ_0 is required ($\vartheta_0 = 30^\circ$) when $\bar{\vartheta} = 0$.

The spectra at 9.3 GHz also show distinct deviations between calculation and experiment when the applied field is in the plane of the bilayer, $\vartheta' = 90^\circ$. The origin of this discrepancy is discussed later.

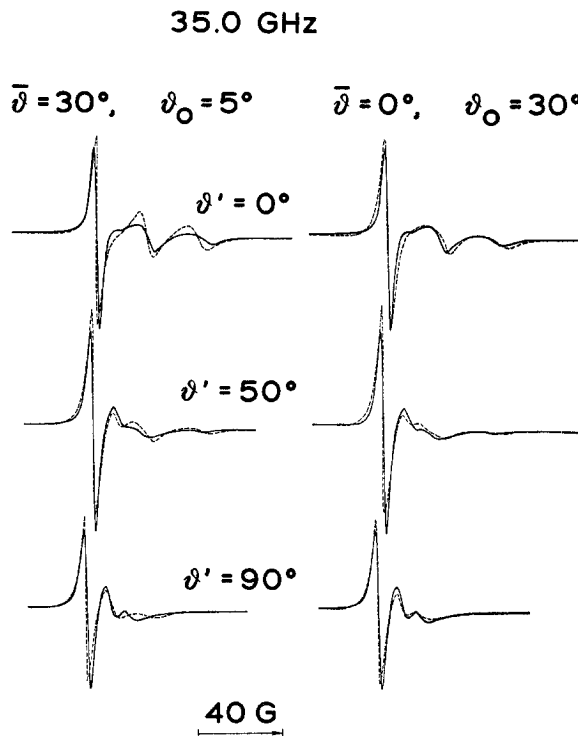


FIG. 7. Comparison of experimental (solid line) and calculated (dashed line) spectra at 35.0 GHz for III(10,3) in hydrated bilayers of egg lecithin. Experimental conditions are similar to those given for Fig. 6 except that the sample is contained between pieces of microscope cover slide ($\sim 1 \times 5$ mm). For calculated spectra approximations A were used and the only parameters differing from those given in Fig. 5 are the magnetic field and peak-to-trough derivative-curve linewidths: $A(1) = 9.0$, $A(0) = 16.8$, $A(-1) = 22.4$ MHz.

The spectra at 35.0 GHz were calculated using the same parameters as at 9.3 GHz, except for the linewidth parameters. The calculated and experimental spectra are shown in Fig. 7. In these spectra the signals are broad and it was not possible to show that the parameters with tilt $\bar{\vartheta} = 30^\circ$, $\vartheta_0 = 5$ provided a better fit than parameters without tilt $\bar{\vartheta} = 0$, $\vartheta_0 = 30^\circ$.

APPROXIMATIONS A'

The same approximations are used as in A except that the φ -dependent distribution function, Eq. [22], is used. Here $\varphi = 0$ is the most probable direction of the projection of z' in the plane perpendicular to N when the applied field has the direction φ' . The parameter φ_0 is infinite when this distribution is cylindrically symmetric, as in Approximations A above. In our samples, this in-plane orientation is evidently field induced (18). The degree of orientation may then depend on the strength of the component of the field that lies in the plane of the phospholipid bilayer; thus, in principle, φ_0 must be considered to be a function of ϑ' and of H_0 . We have only examined the effects of in-plane lipid organization on the spectra for the case where the field lies in the plane of the bilayer, $\vartheta' = 90^\circ$. A striking improvement between calculation and experiment is achieved when φ_0 is taken equal to 30° and the relative field deviation φ' is set equal to 80° , as shown in Fig. 8. The remaining discrepancies between theoretical and experi-

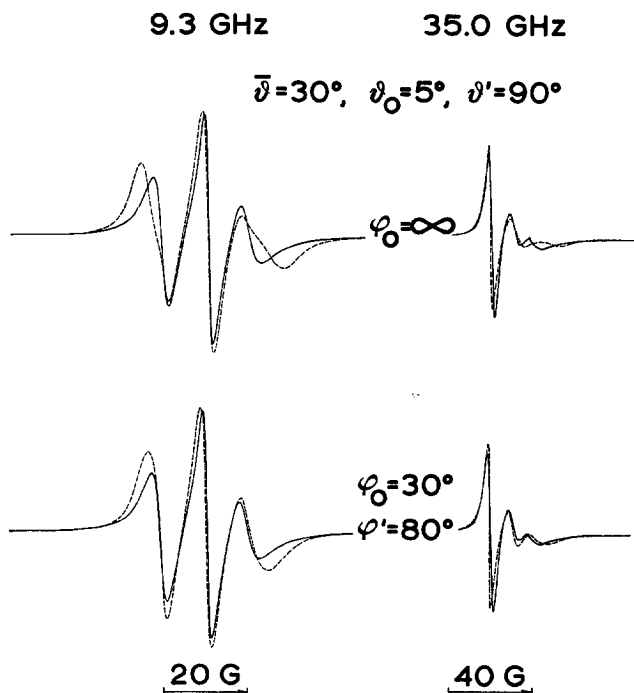


FIG. 8. Calculated and experimental paramagnetic resonance spectra at 9.3 and 35.0 GHz for III(10,3) in oriented multilayers of egg lecithin with the magnetic field perpendicular to the normal to the plane of the glass plates ($H_0 \perp N$) ($\vartheta' = 90^\circ$). Identical experimental spectra (solid line) are shown in Fig. 6. Calculated spectra are shown for both the absence of magnetic field-induced orientation ($\varphi_0 = \infty$) and with magnetic field-induced orientation ($\varphi_0 = 30^\circ$, $\varphi' = 80^\circ$). Approximations A' were used for the calculations. Parameters for the calculation are given in Table 3 and the legend to Fig. 6.

mental spectra, particularly at 9.3 GHz, may be accounted for in terms of angular-dependent linewidth contributions (see Approximations B and B' below).

APPROXIMATIONS B

The same approximations are made as in A except that Approximation (A-3) is replaced by the approximation that the widths of the individual resonance lines are angular dependent, and are given by the following expression:

$$\Delta\nu = A + B[\frac{1}{4}(3 \cos^2 \Theta - 1)^2] + C[3 \cos^2 \Theta \sin^2 \Theta] + D[\frac{3}{4} \sin^4 \Theta]. \quad [23]$$

Here $\Delta\nu$ is the peak-to-trough derivative curve linewidth. Angular-dependent terms of this type arise when the time-dependent perturbation [$\mathcal{H}(t) - \mathcal{H}$] is assumed to have only high-frequency components, and is treated by Redfield theory, assuming \mathcal{H} to have axial symmetry in the T tensor, but not the g-tensor, and assuming \mathcal{H}' to have axial symmetry. This is the same angular-dependent linewidth formula used previously by Gaffney (McFarland) and McConnell (1, 4).

The 9.3-GHz spectra calculated for III(10,3) using these linewidth parameters are shown in Fig. 9a, and the values of these parameters are given in Table 4. As will be seen by comparing Figs. 6 and 9a, the introduction of these linewidth parameters improves the agreement between theory and experiment. The theoretical significance of these parameters is discussed in the Appendix. Even with these parameters, significant discrepancies remain for spectra at $\vartheta' = 90^\circ$.

A clear indication of the necessity of including angular-dependent linewidths is shown by the spectra of III(1,14) given in Fig. 9b. These spectra are simulated essentially perfectly with angular-dependent linewidths. No φ -dependence of the distribution function can be detected here, that is, no effect of field-induced lipid orientation or the orientation or motion of the nitroxide group in III(1,14) can be detected. This is not surprising since this motion is nearly isotropic.

TABLE 4
LINewidth PARAMETERS IN MHz (APPROXIMATIONS B)^a

| | III(10,3) | III(7,6) | III(5,10) | III(1,14) |
|---|-----------------|----------------|---------------|---------------|
| <u>9.3 GHz</u> | | | | |
| <i>A</i> (1), <i>A</i> (0), <i>A</i> (-1) | 9.0, 7.0, 12.0 | 7.8, 6.7, 12.6 | 5.6, 5.6, 9.8 | 3.4, 3.5, 5.0 |
| <i>B</i> (1), <i>B</i> (0), <i>B</i> (-1) | 0, 5.6, 0 | 5.6, 5.6, 0 | 7, 2.6, 5.6 | 1.4, 1.1, 2.5 |
| <i>C</i> (1), <i>B</i> (0), <i>B</i> (-1) | 0, 0, 0 | 0, 0, 5.6 | 2.8, 0, 8.4 | 0, 0, 0 |
| <i>D</i> (1), <i>D</i> (0), <i>D</i> (-1) | 0, 0, 0 | 0, 0, 0 | 0, 0, 0 | 0, 0, 0 |
| <u>35.0 GHz</u> | | | | |
| <i>A</i> (1), <i>A</i> (0), <i>A</i> (-1) | 9.0, 16.8, 22.4 | | | 3.9, 5.0, 7.6 |
| <i>B</i> (1), <i>B</i> (0), <i>B</i> (-1) | 0, 0, 0 | | | 0, 1.7, 2.5 |
| <i>C</i> (1), <i>C</i> (0), <i>C</i> (-1) | 0, 0, 0 | | | 0, 0, 0 |
| <i>D</i> (1), <i>D</i> (0), <i>D</i> (-1) | 0, 0, 0 | | | 0, 0, 0 |

^a *A* is an angle-independent linewidth term. *B* is the coefficient of $1/4(3 \cos^2 \Theta - 1)^2$. *C* is the coefficient of $3 \cos^2 \Theta \sin^2 \Theta$. *D* is the coefficient of $3/4 \sin^4 \Theta$. Widths refer to peak-to-trough derivative-curve presentations.

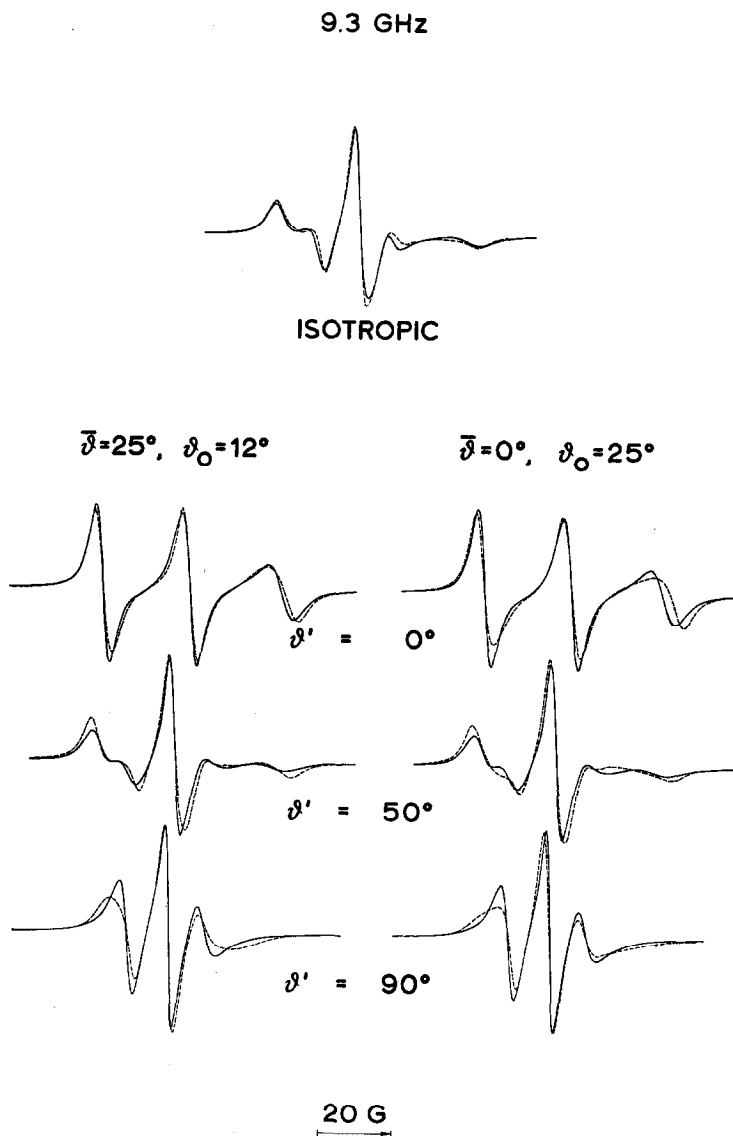


FIG. 9a. Comparison of experimental (solid line) and calculated (dashed line) paramagnetic resonance spectra at 9.3 GHz for III(10,3) in hydrated egg lecithin multilayers. The experimental spectra are identical with those shown in Fig. 6. In this case, Approximations B were used for the calculated spectra. The linewidths for the calculations are given in Table 4. A set of spectra are shown assuming a net tilt of the chain axes ($\bar{\beta} = 25^\circ, \beta_0 = 12^\circ$) and no tilt ($\bar{\beta} = 0^\circ, \beta_0 = 30^\circ$). Three orientations are shown ($\beta' = 0, 50, 90^\circ$).

APPROXIMATIONS B'

The approximations here are the same as in B except that the angular distribution of the z' axis is taken to be that given in Eq. [22]. This approximation with $\varphi_0 = 30^\circ$ and $\varphi' = 80^\circ$ gives excellent agreement between observed and calculated spectra, as shown in Fig. 10.

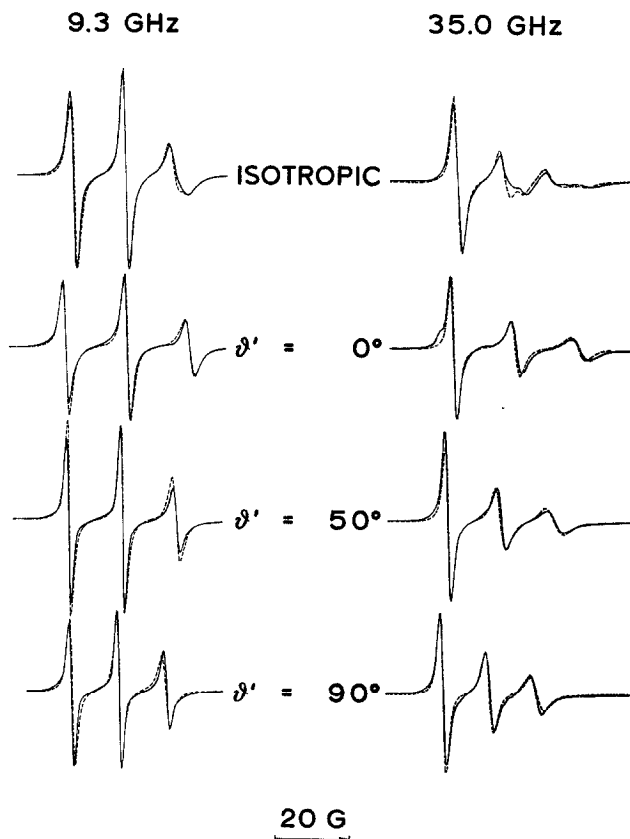


FIG. 9b. Experimental (—) and calculated spectra (----) for III(1,14) in hydrated egg lecithin multilayers at 9.3 and 35.0 GHz. The experimental conditions are described in the legends to Figs. 6 and 7. Approximations B were used for the calculated spectra with the parameters given in Table 3. The linewidths used for the calculations are given in Table 4. No tilt is assumed, $\vartheta_0 = 5^\circ$, and three orientations ($\vartheta' = 0, 50, 90^\circ$) are shown. The apparent discrepancy between calculated and observed spectra in the case of the isotropic 35.0-GHz spectra is probably due to the fact that the "experimental" isotropic spectrum was obtained by appropriate summation of experimental spectra of oriented samples, and an insufficient number of experimental spectra were available.

APPROXIMATIONS C

- (C-1) The effective Hamiltonian \mathcal{H}' does not have axial symmetry either in the \mathbf{g}' or \mathbf{T}' tensor.
- (C-2) The line shape for each hyperfine signal is Lorentzian.
- (C-3) The linewidth for each hyperfine state is isotropic.

In order to study the possible effects of a nonaxially symmetric Hamiltonian, we have considered two extreme cases and only isotropic spectra. In one case, the outer extrema are separated by a hyperfine splitting determined by high-frequency rotations or oscillations about the y -axis (averaging of T_z and T_x) while T_y and g_y are set equal to their fully immobilized values (see Table 1). In the second case, a comparable averaging of T_z and T_y and g_z and g_y is considered. In the first case, $y = y'$, and in the second $x = x'$.

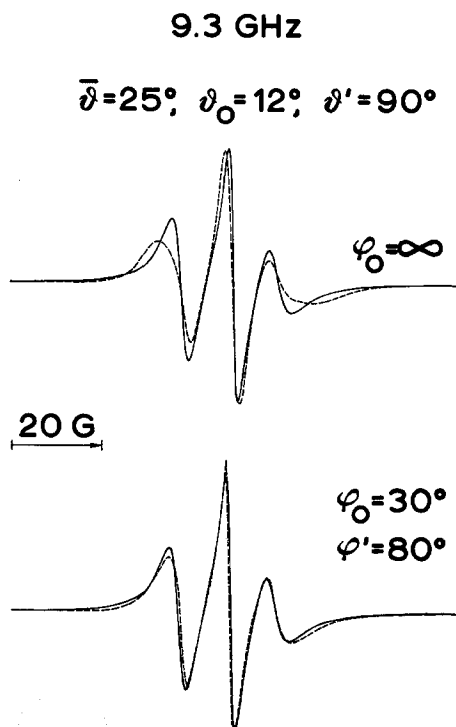


FIG. 10. Experimental and calculated paramagnetic resonance spectra at 9.3 GHz for **III**(10,3) in oriented multilayers of egg lecithin with $H_0 \perp N$ ($\beta' = 90^\circ$). The experimental spectra are identical with those shown in Fig. 6. Calculated spectra were obtained with Approximations B'. Calculated spectra are shown for both the *absence* of magnetic field-induced orientation ($\varphi_0 = \infty$) and *with* magnetic field-induced orientation ($\varphi_0 = 30^\circ, \varphi' = 80^\circ$). Other calculation parameters are the same as those used for Fig. 9a.

Calculated spectra are compared with experimental spectra in Fig. 11 where calculated separations of the outer extrema are set equal to the experimental values. Discrepancies between the two spectra in the case of x -axis rotations (oscillations) are dramatic and rule out this possibility. The disagreement in the case of the y -axis rotation is also pronounced, but we cannot rule out a small contribution of this motion along with the other motions already considered. However, it is clear from consideration of the spectra of Fig. 11 that deviations from axial averaging cannot be large. The observation of a sharp, symmetrical, low-field component of the 35-GHz spectra at all orientations (see Fig. 7) and in the isotropic spectrum obtained by appropriate summation of oriented spectra provides convincing evidence for axial averaging.

THE FLEXIBILITY GRADIENT AND TILT

The paramagnetic resonance spectra of phospholipid labels **III**(m, n) in isotropic distributions of lecithin bilayers are shown in Fig. 12. A semilogarithmic plot of the order parameter $S_{kk'}$ vs. n , the number of methylene groups that separate the oxazolidine ring from the ester carbon atom, is given in Fig. 13. The order parameter $S_{kk'}$, is sometimes designated S_3 (δ) and in the following is referred to briefly as S' . In the present

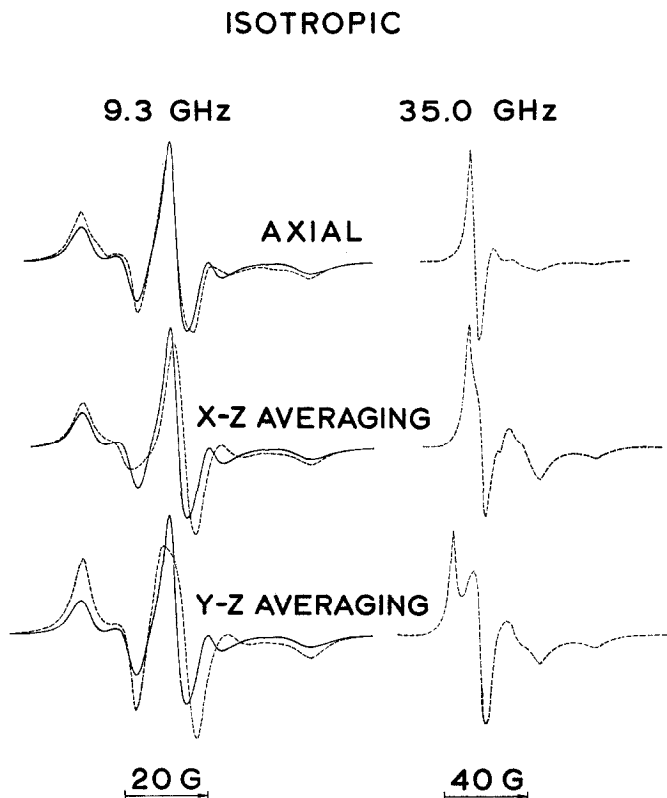


FIG. 11. Isotropic paramagnetic resonance spectra comparing axial averaging with two extreme cases of nonaxial averaging for III(10,3) in hydrated egg lecithin bilayers. Calculated spectra are shown for 9.3 and 35.0 GHz. The experimental isotropic spectrum (solid lines) at 9.3 GHz is superimposed on the calculated spectra (dashed lines). No experimental isotropic spectrum was recorded at 35.0 GHz because of experimental difficulties. The 35.0-GHz spectrum calculated for axial averaging employed parameters which gave a good fit to spectra from an oriented sample (as shown in Fig. 7). At both fields, nonaxial spectra are calculated by assuming that the separation of outer hyperfine extrema is determined by rotations about the y axis (x - z averaging) or about the x axis (y - z averaging). The input parameters for the calculation that assumes axial averaging are given in Table 3 for III(10,3). The input parameters for the nonaxial calculations are, for x - z averaging: $T'_{xx} = 34.64$ MHz, $T'_{yy} = 16.32$ MHz, $T'_{zz} = 76.83$ MHz, $g'_{xx} = 2.00744$, $g'_{yy} = 2.0061$, $g'_{zz} = 2.00406$, and for y - z averaging, $T'_{zz} = 17.67$ MHz, $T'_{yy} = 33.29$ MHz, $T'_{xx} = 76.83$ MHz, $g'_{xx} = 2.0088$, $g'_{yy} = 2.00536$, $g'_{zz} = 2.00346$. Peak-to-trough derivative linewidths for all calculated spectra at 9.3 GHz are $A(1) = 9.8$, $A(0) = 9.8$, $A(-1) = 14$ MHz, and at 35.0 GHz, $A(1) = 9.0$, $A(0) = 16.8$, $A(-1) = 22.4$ MHz.

work, S' is calculated using the following equation, which includes a solvent polarity correction as discussed previously (3, 6).

$$S' \simeq \left(\frac{T'_{\parallel} - T'_{\perp}}{T_{zz} - T_{av}} \right) \left(\frac{a}{a'} \right), \quad [24]$$

$$a = \frac{1}{3} \text{Trace}(\mathbf{T}), \quad [25]$$

$$T_{av} = \frac{1}{2}(T_{xx} + T_{yy}). \quad [26]$$

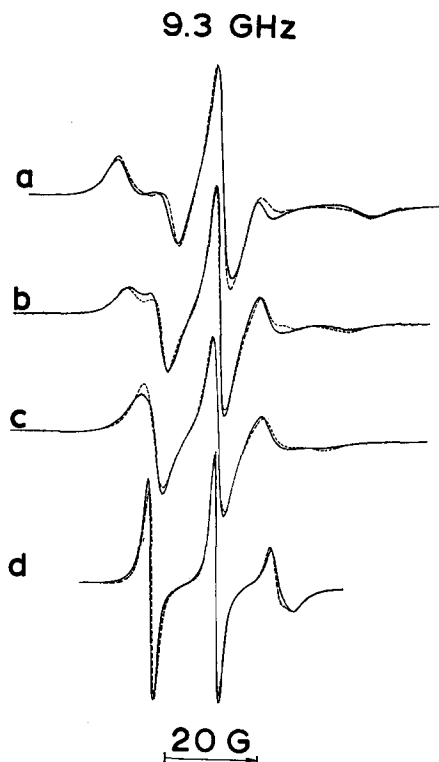


FIG. 12. Isotropic paramagnetic resonance spectra at 9.3 GHz for phospholipid labels $\text{III}(m,n)$ in hydrated bilayers of egg lecithin (see Fig. 6 legend for experimental details). Calculated spectra (dashed lines) are superimposed on experimental spectra (solid lines) for labels a, $\text{III}(10,3)$; b, $\text{III}(7,6)$; c, $\text{III}(5,10)$, and d, $\text{III}(1,14)$. Input parameters for the calculations are given in Tables 3 and 4.

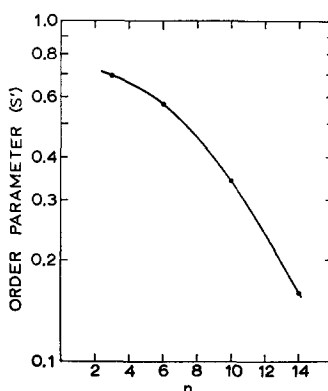


FIG. 13. Semilogarithmic plot of the order parameter (S') as a function of n for spin labels $\text{III}(m,n)$ in isotropic distributions of bilayers of hydrated egg lecithin. The paramagnetic resonance spectra for these spin labels in egg lecithin are shown in Fig. 12. The order parameters were calculated using Eq. [24], the values of T'_1 and T_\perp given in Table 3 and values of T_{xx} , T_{yy} , T_{zz} given in Table 1.

In recent work it has been possible to determine order parameters from quadrupole splittings in the deuterium nuclear resonance spectra of selectively deuterium-labeled fatty acid chains (19). These order parameters are nearly constant at various positions along the fatty acid chains, except near the terminal methyl groups.

In general, order parameters represent certain time averages over molecular motion. The longer the time involved in the averaging, the lower the order parameter. The time involved in the averaging depends on the magnitudes of the anisotropies of terms in the spin Hamiltonian. In our case, this involves hyperfine and g -factor interactions, and in the case mentioned above, it involves deuterium electric quadrupole interactions.

To facilitate the comparison of order parameters from the two measurements, let us calculate the values of the hyperfine splittings, T''_{\parallel} and T''_{\perp} , that would be observed if the lifetime of the statistically tilted chain regions were short compared to $T'_{\parallel} - T'_{\perp}$, and $(g'_{\parallel} - g'_{\perp})|\beta|H_0/h$. That is, for the purposes of this discussion, let us consider a hierarchy of molecular motions, those which are very fast and yield the effective Hamiltonian \mathcal{H}' , and then a hypothetical additional fast motion yielding a second effective Hamiltonian \mathcal{H}'' . Assume that these additional motions correspond to the motion of z' such that $\vartheta = \vartheta(t)$ and $\varphi = \varphi(t)$ (the polar and azimuthal angles of z' relative to the bilayer normal \mathbf{N} and an arbitrary direction fixed in the bilayer plane). The new order parameter S'' can be related to the old order parameter S' as follows:

$$S'' = \frac{T''_{\parallel} - T''_{\perp}}{T_{zz} - T_{av}}, \quad [27]$$

$$S'' = \left(\frac{T''_{\parallel} - T''_{\perp}}{T'_{\parallel} - T'_{\perp}} \right) \left(\frac{T'_{\parallel} - T'_{\perp}}{T_{zz} - T_{av}} \right), \quad [28]$$

$$S'' = fS', \quad [29]$$

where

$$f = \overline{\frac{1}{2}(3 \cos^2 \vartheta - 1)}. \quad [30]$$

In terms of our previously derived parameters,

$$f = \frac{\int_0^{\pi} \frac{1}{2}(3 \cos^2 \vartheta - 1) \exp - [(\vartheta - \bar{\vartheta})^2/2\vartheta_0^2] \sin \vartheta d\vartheta}{\int_0^{\pi} \exp - [(\vartheta - \bar{\vartheta})^2/2\vartheta_0^2] \sin \vartheta d\vartheta}. \quad [31]$$

Table 5 gives estimates of f and S'' for three phospholipid spin labels.

TABLE 5

| Phospholipid spin label | Order parameter S' | f | Order parameter S'' | Ensemble average order parameter |
|-------------------------|----------------------|------|-----------------------|----------------------------------|
| (10,3) | 0.69 | 0.62 | 0.41 | 0.43 |
| (5,10) | 0.34 | 0.88 | 0.30 | 0.30 |
| (1,14) | 0.16 | 0.98 | 0.16 | 0.16 |

It will be seen that the order parameter S'' (and also the ensemble average order parameter discussed later) shows a lower gradient of order towards the terminal methyl

group. Thus, the quadrupole splitting data that show a constancy of order parameters are not as inconsistent with the spin-label data as they might appear to be at first glance. On the other hand, quantitative identity of the order parameters for S'' and the quadrupole order parameter is obviously not to be expected.

The lifetime of the statistically tilted chain regions may be just long enough for tilt to be observed with spin labels. This possibility is suggested by the known high rates of lateral diffusion (9-13) which should be effective in averaging out tilt *if* the diffusion is isotropic in the plane of the bilayer. One of the manifestations of tilt in the paramagnetic resonance spectra of III(10,3) in lecithin bilayers is that the separation between the

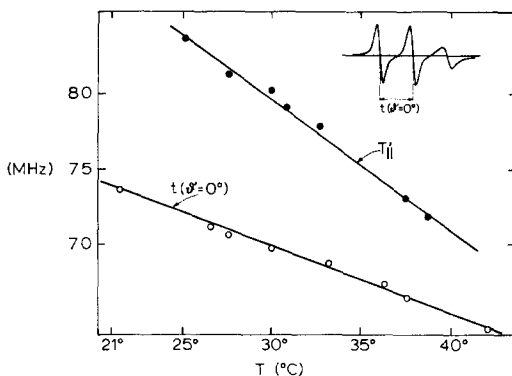


FIG. 14. The temperature dependence of $T'_{||}$ derived from spectra of isotropic samples and the separation of the $m = 1$ and $m = 0$ lines of the $\vartheta' = 0^\circ$ oriented sample for III(10,3) in hydrated bilayers of egg lecithin-cholesterol (2:1) containing 1 mole % of the spin label. Temperature was varied by a flow of heated, hydrated nitrogen. The nonequality of $T'_{||}$ and $t(\vartheta' = 0^\circ)$ is directly due to tilting of the π -orbital axis (z' -axis).

$m = 1$ and $m = 0$ lines ($t(\vartheta' = 0^\circ)$) in the oriented sample for $\vartheta' = 0^\circ$ is smaller than the value of $T'_{||}$ obtained from an isotropic sample. We find that the magnitude of this difference decreases with increasing temperature, as shown in Fig. 14. Thus, the lifetime of the net tilt may not be very long compared to $T'_{||} - t(\vartheta' = 0^\circ)$ at the high temperatures. Alternatively, the temperature dependence of $\bar{\vartheta}$ and ϑ_0 may be responsible for this observed temperature effect. It should be noted here that although a large spread of distributions of chain orientations (ϑ_0 large) but zero tilt parameter ($\bar{\vartheta} = 0^\circ$) would also make $t(\vartheta' = 0^\circ)$ smaller than $T'_{||}$, we do not believe that this situation accounts for the observed spectra. This conclusion results from the fact that the experimental $\vartheta' = 0^\circ$ spectrum is quite symmetrical and the separation of $m = 1$ and $m = 0$ lines is practically identical to the separation of the $m = 0$ and $m = -1$ lines. As shown in Figs. 6 and 9a, large ϑ_0 contributions lead to unsymmetrical spectra at $\vartheta' = 0^\circ$.

ENSEMBLE DISTRIBUTION FUNCTION

Another approach that can be used for comparing the results of spin label experiments with other spectroscopic data is to calculate an ensemble distribution function $\rho_e(\vartheta_i)$, where $\rho_e(\vartheta_i)d\vartheta_i$ gives the ensemble average probability that at any instant of time a principal axis z (the π -orbital axis) can be found between ϑ_i and $\vartheta_i + d\vartheta_i$. No

field-induced orientation is taken into account in the present calculation, and the ensemble is assumed to be sufficiently large that there is no collective tilt in any one direction. Thus $\rho_e(\vartheta_i)$ is cylindrically symmetric about the normal to the bilayer plane.

The ensemble distribution function $\rho_e(\vartheta_i)$ is a convolution of two distribution functions, the average axis distribution function $\rho(\vartheta)$ discussed earlier, Eq. [21], and an instantaneous distribution function $\rho_i(\Theta, \Phi)$ that gives the instantaneous orientation of a hyperfine axis z in the average axis system z', x', y' . The probable values of ϑ_i are defined by the probable values of Θ, Φ, ϑ and φ . Since the distribution of z' about \mathbf{N} is axially symmetric, ϑ_i is given by the following equation:

$$\cos \vartheta_i = \cos \Theta \cos \vartheta + \sin \Theta \sin \vartheta \cos \Phi. \quad [32]$$

The distribution function $\rho_e(\vartheta_i)$ is then given by the convolution integral,

$$\rho_e(\vartheta_i) = \int_0^\pi \rho(\vartheta) d\vartheta \int_0^\pi d\Theta \int_0^{2\pi} d\Phi \rho_i(\Theta, \Phi) \sin \vartheta_i \delta(\cos \vartheta_i - \cos \Theta \cos \vartheta - \sin \Theta \sin \vartheta \cos \Phi). \quad [33]$$

This integral can be rewritten:

$$\rho_e(\vartheta_i) = 2 \int_0^\pi \int_0^\pi \frac{\rho(\vartheta) \rho_i(\Theta) d\Theta d\vartheta \sin \vartheta_i}{(\sin^2 \Theta \sin^2 \vartheta - (\cos \vartheta_i - \cos \Theta \cos \vartheta)^2)^{1/2}} \quad [34]$$

by using the following general property of δ -functions:

$$\int_0^{2\pi} \delta(a + b \cos x) dx = \frac{2}{(b^2 - a^2)^{1/2}}. \quad [35]$$

We have analyzed our data in terms of a distribution function having an axially symmetric Gaussian form

$$\rho_i(\Theta, \Phi) = \frac{1}{2\pi} \sin \Theta \exp(-\Theta^2/2\Theta_0^2), \quad [36]$$

where the width parameter Θ_0 is determined from the observed order parameter by the equation

$$S' = \frac{1}{2} \frac{\int_0^\pi \sin \Theta \exp[-\Theta^2/2\Theta_0^2] (3 \cos^2 \Theta - 1) d\Theta}{\int_0^\pi \sin \Theta \exp[-\Theta^2/2\Theta_0^2] d\Theta}. \quad [37]$$

Plots of the calculated distribution function $\rho_e(\vartheta_i)$ for the labels **III**(1,14) and **III**(10,3) are given in Fig. 15, using the Gaussian approximation in Eq. [36]. It will be seen that these distribution functions exhibit distinct maxima, showing that there is a significant tilt of the instantaneous orientation of the z -axis. In the cases of **III**(10,3), distinct maxima are also observed in plots of $\rho(\vartheta_i)/\sin \vartheta_i$.

Although we have calculated the distribution functions $\rho_e(\vartheta_i)$ using Eq. [34], the plots given in Fig. 15 were in fact obtained from a tedious but more direct computer calculation. Values for Θ, ϑ , and Φ were chosen at 1° intervals, and for each triplet of these values a value of ϑ_i was calculated using Eq. [32]. The "allowed" values of ϑ_i so calculated were then sorted into 1° intervals and the products $\rho(\vartheta)\rho_i(\Theta, \Phi)$ summed for each

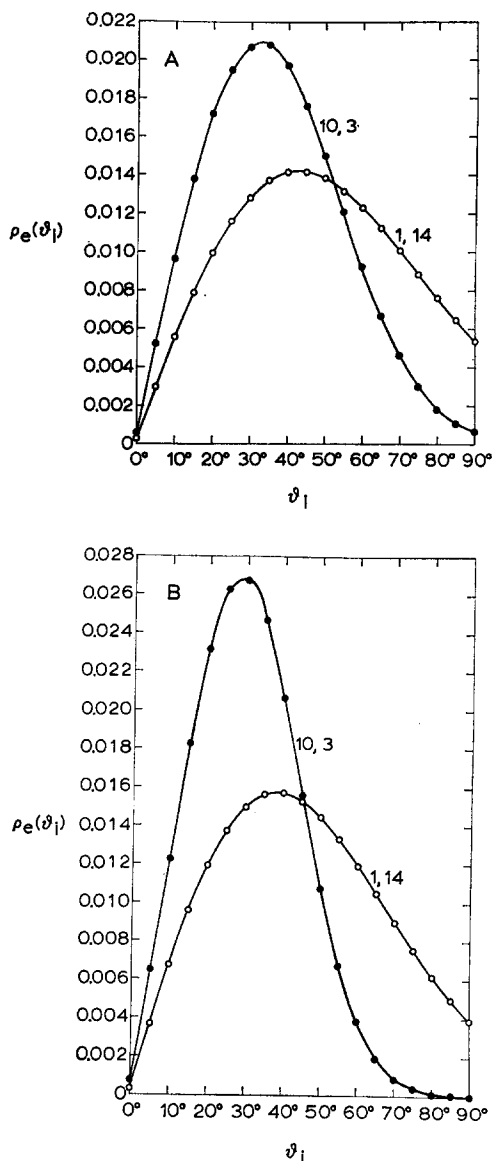


FIG. 15. Plots of the function $\rho(\vartheta_1)$ vs. ϑ_1 for (a) hydrated bilayers of egg lecithin and (b) egg lecithin-cholesterol bilayers (2:1 mole ratio). Plots for labels III(10,3) (●—●) and label III(1,14) (○—○) are included. For the plot of III(10,3) data, in egg lecithin, $\bar{\vartheta} = 30^\circ$, $\vartheta_0 = 5^\circ$, $\Theta_0 = 21^\circ$, $S' = 0.69$; in egg lecithin-cholesterol, $\bar{\vartheta} = 25^\circ$, $\vartheta_0 = 5^\circ$, $\Theta_0 = 16^\circ$, $S' = 0.79$. For the plot of III(1,14) data, in egg lecithin $\bar{\vartheta} = 0^\circ$, $\vartheta_0 = 5^\circ$, $\Theta_0 = 48^\circ$, $S' = 0.16$; in egg lecithin-cholesterol, $\bar{\vartheta} = 0^\circ$, $\vartheta_0 = 5^\circ$, $\Theta_0 = 42^\circ$, $S' = 0.23$.

interval. The two methods of calculation gave similar results, but the procedure used to obtain the plots in Fig. 15 avoided computational uncertainties involving singularities in the integrand of Eq. [34]. The data in Fig. 15 are accurate to within a few percent.

As mentioned later in the Discussion, from a biophysical point of view, the fact that the π -orbital is tilted is less significant than the fact that the tilt can be detected in the

paramagnetic resonance spectra. This result demonstrates unequivocally that there is a relatively long-lived collective structure in the polar head group region of the non-spin-label phospholipid molecules that is not averaged out by rapid molecular motion (in contrast to the absence of any such long-lived structure near the terminal methyl groups in fluid lipid domains (4)).

Values of the ensemble average order parameters are also given in Table 5. These order parameters are the average of $\frac{1}{2}(3\cos^2\vartheta_i - 1)$ over the distribution function $\rho_e(\vartheta_i)$. As expected, these order parameters are essentially equal to the double time-average order parameters S'' calculated in the previous section and given in Table 5.

FIELD-INDUCED ORIENTATION AND LIPID DOMAINS

The present paper summarizes spin-label evidence for field-induced lipid orientation, which has been reported briefly earlier (18). This earlier report also provides optical evidence for a field-induced lipid orientation. Presumably lipid molecules in the bilayers are organized into domains that have an appreciable diamagnetic anisotropy, and it is these domains containing large numbers of molecules that are responsive to the applied field.

In the present work we have found that the parameters $\varphi' = 80^\circ$ and $\varphi_0 = 30^\circ$ in the distribution function give good simulation of the observed spectra when the applied field is in the plane of the lipid bilayer. It should be noted that there are certain equivalent orientations of the preferred z' -axis direction in the plane that are magnetically equivalent to $\varphi = 0$ and may be assumed to be present in the sample. One equivalent direction corresponds to a twofold rotation of the molecules about the field direction, and the other is equivalent to a reversal of the field direction.

In the optical studies indicating a field-induced birefringence in the sample, evidence was obtained that the induced birefringence was roughly proportional to the applied field strength, at least for field strengths up to 35,000 gauss (18). It is therefore likely that the parameter φ_0 , which should reflect the degree of field-induced lipid orientation, should be dependent on the strength of the applied field \mathbf{H}_0 and the angle ϑ' between \mathbf{H}_0 and \mathbf{N} . In our simulations of spectra, we have not attempted to include the possible field dependence of φ_0 .

DISCUSSION

This paper summarizes a number of rather elaborate calculations we have made concerning the analysis of the paramagnetic resonance spectra of phospholipid spin labels incorporated in phospholipid bilayer membranes. Because our analysis of the resonance spectra of spin labels is directed towards the study of biophysical problems, one may question the value of these elaborate calculations, since the paramagnetic nitroxide group is not a natural component of biological systems and is always to some extent a perturbation on the system of immediate biophysical interest. We summarize here arguments that this detailed analysis is indeed justified.

Quantitative analyses of the spectra of spin-labeled phospholipids have led to some conclusions that are totally free of uncertainties concerning structural perturbations by the paramagnetic nitroxide group. For example, the long-lived static tilt of the effective hyperfine axis z' reported here and earlier (4, 5) proves conclusively that there must be a relatively rigid, collective structure of the phospholipids near the polar head group

region with a lifetime of at least 10^{-7} – 10^{-8} sec; otherwise this tilt would be averaged to zero by rapid molecular motions involving the spin label and the surrounding lipid molecules. The same general argument can be made regarding the evidence for an in-plane magnetic-field-induced orientation of the phospholipid molecules. Obviously there is no significant direct effect of an applied field on the orientation of a single spin-labeled phospholipid molecule. Further, the spectra show clearly that the labels are present in dilute solution since there is no detectable spin–spin interaction. Thus, the field is not acting on a domain rich in spin-labeled lipids. The field-induced lipid orientation (detected originally by this quantitative analysis of the spin-label phospholipid paramagnetic resonance spectra) must be a property of the host lipid matrix itself. In other studies of phospholipid membranes using spin labels, the rates of phospholipid “flip-flop” (inside–outside transition (14)), the rates of lateral diffusion (9–13) and lateral phase separations (20, 21), similar arguments can be made as to the general validity of the results.

Probably the case where the spin-labeled phospholipids and their “perturbation-free” counterparts (deuterium-labeled phospholipids or fatty acids) show the largest difference is in the order parameters. In the case of the spin-labeled phospholipids, there is a distinct decrease in order parameter towards the terminal methyl groups, whereas the deuterium resonance spectra exhibit quadrupole splittings that yield a relatively constant order parameter except very close to the terminal methyl group (19). Some of this difference may obviously arise from the nitroxide group structural perturbation, but, as emphasized in earlier sections of this paper, there are good reasons to believe that some of this discrepancy is due to a more interesting effect, namely, the spin-label spectra and deuterium resonance spectra reflect different time averages over molecular motions.

Our conclusion is that detailed, quantitative analyses of the resonance spectra of spin-labeled molecules in membranes are indeed justified in spite of possible significant perturbations of the nitroxide group in some but not all cases. Additional new properties of membranes may be discovered using this quantitative analysis of the resonance spectra.

APPENDIX: REDFIELD RELAXATION

In previous work we used Redfield theory to show that the time-dependent term [$\mathcal{H}(t) - \mathcal{H}'$] yields angular dependent linewidths having the general form shown in Eq. [23]. Observed resonance spectra were then analyzed, treating A , B , C , and D as purely empirical parameters, in the same way that these parameters have been treated in the present paper. More recently, Schindler and Seelig used a similar but somewhat more general version of Redfield theory with impressive success to analyze the resonance spectra of the fatty acid labels $\text{II}(m,n)$ in smectic liquid crystals composed of mixtures of decanol and sodium decanoate (7). In their work they used this theory to interpret parameters such as A , B , C , D in Eq. [23] in terms of correlation times and activation energies for chain motion. Hemminga and Berendsen (22) have also used a version of Redfield theory to study the spectra of a cholesterol spin label in bilayers. These authors did not employ distribution functions of type $\rho(\vartheta)$. Another interesting treatment of the angular dependence of paramagnetic resonance spectra of label I in smectic liquid crystals has been given by Luckhurst *et al.* (23). The liquid-crystal system used in this case is different from the liquid crystals employed by Seelig and coworkers (7) and is

also different from our phospholipid bilayer system, so it is not possible to compare the results of the three treatments directly. Unfortunately, in the cases of greatest interest to us, namely the phospholipid labels **III**(m, n) in phospholipid bilayers, it is particularly difficult to prove the adequacy of Redfield theory because of the large inhomogeneous linewidth contributions and also because of the field-induced lipid orientation. However, as discussed below, in at least one case (**III**(1,14)) our observed spectra provide very convincing evidence for the adequacy of Redfield theory in accounting for relative linewidths and their field dependence. The following expression (Eq. [38]) gives the Lorentzian contribution to the resonance linewidths using Redfield theory (4):

$$\begin{aligned}
 1/T_2 = (2\pi)^2 \left\{ \sum_{q=0, \pm 1, \pm 2} (\overline{|D_{0q}|^2} - |\overline{D_{0q}}|^2) \frac{1}{2} v_e G_0(\mathbf{h} \cdot \mathbf{T}'_q \cdot \mathbf{h}) + A_0(\mathbf{h} \cdot \mathbf{T}'_q \cdot \mathbf{k}'')^2 \tau_{0q} \right. \\
 + \sum_{\substack{n \neq 0 \\ q=0, \pm 1, \pm 2}} G_n^2 \overline{|D_{nq}|^2} \frac{1}{4} v_e^2 |\mathbf{h} \cdot \mathbf{T}'_q \cdot \mathbf{h}|^2 \tau_{nq} \\
 \left. + \frac{1}{4} (2 - m^2) A_0^2 \sum_{q=0, \pm 1, \pm 2} (\overline{|D_{0q}|^2} - |\overline{D_{0q}}|^2) |\mathbf{h} \cdot \mathbf{T}'_q \cdot \mathbf{v}^+|^2 (\tau_{0q}) / (1 + \tau_{0q}^2 \omega^2) \right\}. \quad [38]
 \end{aligned}$$

(In our earlier report (4), we omitted the pseudosecular term for brevity, since it did not introduce any new terms into the form of Eq. [23].) In the pseudosecular term, ω is the angular resonance frequency of the nitrogen nucleus in the nitrogen nuclear hyperfine field.

For simplicity, deviations of the hyperfine tensor \mathbf{T} from axial symmetry have been neglected, as have nonsecular terms (except for the pseudosecular term). (For more general expressions, see Schindler and Seelig (7).) We neglect the nonsecular terms primarily on experimental grounds. Spin packet T_2 's for nitroxide spin labels are usually shorter than the corresponding T_1 's, except for the very smallest labels in liquids of low viscosity. The deviation of \mathbf{T} from axial symmetry is small, and the neglect of this deviation cannot seriously affect any of our conclusions. The Wigner rotation matrices $D_{mq} \equiv D_{mq}^{(2)}(\alpha\beta\gamma)$ are the same as those given by Saha and Das (24) and $\overline{|D_{mq}|^2}$ and $|\overline{D_{mq}}|^2$ are appropriate time averages over the presumed rapid motion of the x, y, z axis system relative to the x', y', z' axis system. In the above equation, $\mathbf{v}^+ = \mathbf{i}'' + \sqrt{-1}\mathbf{j}''$ and \mathbf{k}'' is a unit vector in the direction of the local field acting at the nitrogen nuclear spin. This vector lies in the plane of \mathbf{h} and \mathbf{k}' , and $\mathbf{h} \cdot \mathbf{k}' = \cos \Theta'$, where

$$\cos \Theta' = \frac{\cos^2 \Theta T'_\parallel + \sin^2 \Theta T'_\perp}{(\cos^2 \Theta T'^2_\parallel + \sin^2 \Theta T'^2_\perp)^{1/2}}. \quad [39]$$

In Approximations B, we have used angular-dependent linewidths arising from the various terms that appear in Eq. [38] above, except that we have everywhere replaced \mathbf{k}'' by \mathbf{k}' . This amounts to assuming that $\cos \Theta'$ is equal to one, which is certainly not true for some labels and some angles. For this reason we give in Fig. 16 a plot of Θ' vs. Θ for **III**(10,3) and **III**(1,14), which illustrates the maximum range of this equation.

The 9.3-GHz and 35.0-GHz spectra of the phospholipid label **III**(1,14) are nearly isotropic, as can be seen in Fig. 9b. The adequacy of Redfield theory in accounting for the *relative* linewidths observed in these spectra can be seen immediately by considering the following simplification of Eq. [38], appropriate to isotropic motion, together with

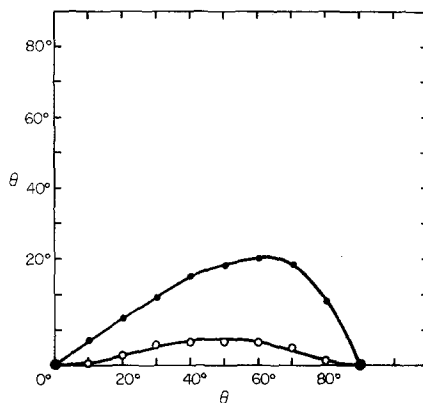


FIG. 16. A plot of θ' vs. θ for labels $\text{III}(10,3)$ (\bullet — \bullet) and $\text{III}(1,14)$ (\circ — \circ). Equation [39] gives the relationship between θ' and θ .

the known values of the parameters, $G_0 = -0.00194$, $A_0 = 31.35$ MHz, and $G_2 = 0.000675$:

$$\frac{1}{T_2} = \frac{(2\pi)^2}{5} \left[\frac{8}{3} (\frac{1}{2} v_e G_0 + A_0 m)^2 \tau + \frac{2}{3} v_e^2 G_2^2 \tau + (2 - m^2) A_0^2 \left(\frac{\tau}{1 + \omega^2 \tau^2} \right) \right]. \quad [40]$$

The Redfield theory accounts quantitatively for the linewidth differences. That is, if one removes the inhomogeneous contributions to the linewidths by calculating differences in peak-to-trough separations, such as $\Delta\nu(m=0) - \Delta\nu(m=1)$, and equates such differences to $1/\pi\sqrt{3}T_2(m=0) - 1/\pi\sqrt{3}T_2(m=1)$, then essentially all of the differences $\Delta\nu(m') - \Delta\nu(m'')$ at both 9.3 and 35.0 GHz can be accounted for in terms of the

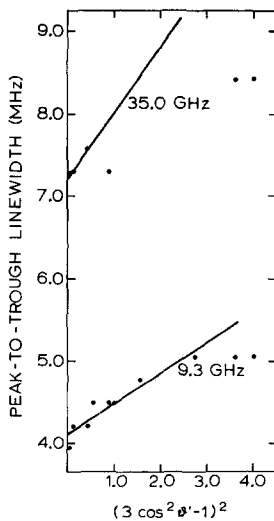


FIG. 17. The experimental peak-to-trough derivative curve linewidths of the center ($m=0$) line for phospholipid label $\text{III}(1,14)$ in oriented bilayers of hydrated egg lecithin vs. $(3 \cos^2 \theta' - 1)^2$ (θ' is defined in Fig. 5). The results of experiments at two fields, 9.3 and 35.0 GHz, are given.

above values of the parameters and a value of τ of $\sim 0.2 \times 10^{-9}$ sec. This value of τ is accurate to within a factor of two and is close to the correlation time determined by Schindler and Seelig (7). This value of τ is consistent with the neglect of the nonsecular relaxation terms. Further refinements can be made to take into account the small anisotropy of the motion and are indicated by the parameters given in Tables 3 and 4. The same correlation time is applicable. (A treatment of line shapes specifically concerned with rapid molecular motion in weakly anisotropic media has been given by Kuznetsov and Lifshits (25). This calculation should be applicable to the spectra of **III**(1,14).)

The B term in Eq. [23] appears to be the largest among the angular-dependent terms. Plots of derivative curve peak-to-trough line separations of the middle ($m = 0$) lines of the resonance spectra in oriented samples are given in Fig. 17 for **III**(1,14) at 9.3 and

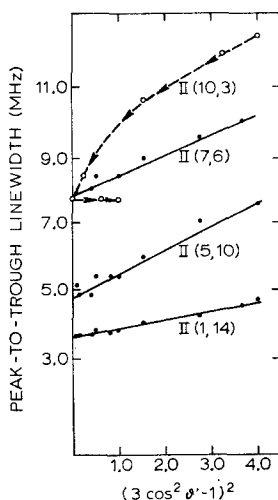


FIG. 18. The experimental peak-to-trough derivative-curve linewidths of the center line ($m = 0$) for fatty acid labels **II**(m, n) in oriented bilayers of hydrated egg lecithin vs. $(3 \cos^2 \theta' - 1)^2$. Experiments were performed at 9.3 GHz.

35.0 GHz, and in Fig. 18 for different fatty acids **II**(m, n) in lipid bilayers. The linewidths of the spectra of fatty acid labels are included since they more clearly show the $(3 \cos^2 \theta - 1)^2 (\simeq (3 \cos^2 \theta' - 1)^2)$ dependence. In the case of the other phospholipid labels, there is less direct evidence for the adequacy of Redfield theory, but we have no reason to doubt its applicability.

ACKNOWLEDGMENT

We are indebted to Professor M. H. F. Wilkins and Dr. Y. K. Levine for stimulating correspondence concerning distribution functions for fatty acid chains in phospholipid bilayers. We are also grateful to Dr. George Gaffney who provided much help with the δ -function calculation used for one calculation of the ensemble distribution function, and to Jim Crapuchettes and Clark Thompson for developing the computer program used for the second method for calculating the ensemble distribution function. This research has been sponsored by the National Science Foundation (Grant No. GB 33501X1) and has benefited from facilities made available to Stanford University by the Advanced Research Projects Agency through the Center for Material Research.

REFERENCES

1. For recent reviews see: B. J. GAFFNEY, in "Methods in Enzymology" (S. Fleischer, L. Packer, and R. W. Estabrook, Eds.), Vol. 32, Academic Press, New York (in press); P. JOST, A. S. WAGGONER, AND O. H. GRIFFITH, in "Structure and Function of Biological Membranes" (L. I. Rothfield, Ed.), p. 83, Academic Press, New York, 1971; I. C. P. SMITH, in "Biological Applications of Electron Spin Resonance Spectroscopy" (J. R. Bolton, D. Borg, and H. Swartz, Eds.), Wiley Interscience, New York, 1972; J. SEELIG, in "Biomembranes", 3 (L. A. Manson, Ed.), p. 267, Plenum Press, New York, 1972.
2. W. L. HUBBELL AND H. M. MCCONNELL, *Proc. Nat. Acad. Sci. USA* **61**, 12 (1968).
3. W. L. HUBBELL AND H. M. MCCONNELL, *J. Amer. Chem. Soc.* **93**, 314 (1971).
4. B. G. MCFARLAND AND H. M. MCCONNELL, *Proc. Nat. Acad. Sci. USA* **68**, 1274 (1971).
5. H. M. MCCONNELL AND B. G. MCFARLAND, *Ann. N.Y. Acad. Sci.* **195**, 207 (1972).
6. J. SEELIG, *J. Amer. Chem. Soc.* **92**, 3881 (1970).
7. H. SCHINDLER AND J. SEELIG, *J. Chem. Phys.* **59**, 1841 (1973).
8. P. JOST, L. J. LIBERTINI, V. C. HEBERT, AND O. H. GRIFFITH, *J. Mol. Biol.* **59**, 77 (1971).
9. P. DEVAUX AND H. M. MCCONNELL, *J. Amer. Chem. Soc.* **94**, 4475 (1972).
10. H. TRÄUBLE AND E. SACKMANN, *J. Amer. Chem. Soc.* **94**, 4499 (1972).
11. C. J. SCANDELLA, P. DEVAUX, AND H. M. MCCONNELL, *Proc. Nat. Acad. Sci. USA* **69**, 2056 (1972).
12. P. DEVAUX, C. J. SCANDELLA, AND H. M. MCCONNELL, *J. Magn. Resonance* **9**, 474 (1973).
13. R. D. KORNBERG AND H. M. MCCONNELL, *Proc. Nat. Acad. Sci. USA* **68**, 2564 (1971).
14. R. D. KORNBERG AND H. M. MCCONNELL, *Biochemistry* **10**, 1111 (1971).
15. H. M. MCCONNELL AND B. G. MCFARLAND, *Quart. Rev. Biophys.* **3**, 91 (1970).
16. A. G. REDFIELD, *IBM J. Res. Develop.* **1**, 19 (1957).
17. R. C. MCCALLEY, E. J. SHIMSHICK, AND H. M. MCCONNELL, *Chem. Phys. Letters* **13**, 115 (1972); C. F. POLNASZEK, G. V. BRUNO, AND J. H. FREED, *J. Chem. Phys.* **58**, 3185 (1973).
18. B. J. GAFFNEY AND H. M. MCCONNELL, *Chem. Phys. Letters*, **24**, 310 (1974).
19. J. CHARVOLIN, P. MANNEVILLE, AND B. DELOCHE, *Chem. Phys. Letters* **23**, 345 (1973). Also, J. SEELIG AND A. SEELIG, *BBRC*, in press.
20. E. J. SHIMSHICK AND H. M. MCCONNELL, *Biochemistry* **12**, 2351 (1973).
21. E. J. SHIMSHICK AND H. M. MCCONNELL, *BBRC* **53**, 446 (1973).
22. M. A. HEMMINGA AND H. J. C. BERENDSEN, *J. Magn. Resonance* **8**, 77 (1972).
23. G. R. LUCKHURST, M. SETAKA, AND C. ZANNONI, *Mol. Phys.*, in press.
24. A. K. SAHA AND T. P. DAS, "Theory and Applications of Nuclear Induction," Saha Institute of Nuclear Physics, Calcutta, 1957.
25. A. N. KUZNETSOV AND V. A. LIFSHITS, *Chem. Phys. Letters* **20**, 534 (1973).